

Alternating current stimulation entrains and connects cortical regions in a neural mass model*

Alexander Pei¹ and Barbara G. Shinn-Cunningham^{1,2}

Abstract—Transcranial alternating current stimulation (tACS) is a neuromodulatory technique that is widely used to investigate the functions of oscillations in the brain. Despite increasing usage in both research and clinical settings, the mechanisms of tACS are still not completely understood. To shed light on these mechanisms, we injected alternating current into a Jansen and Rit neural mass model. Two cortical columns were linked with long-range connections to examine how alternating current impacted cortical connectivity. Alternating current injected to both columns increased power and coherence at the stimulation frequency; however this effect was greatest at the model's resonant frequency. Varying the phase of stimulation impacted the time it took for entrainment to stabilize, an effect we believe is due to constructive and destructive interference with endogenous membrane currents. The power output the model also depended on the phase of the stimulation between cortical columns. These results provide insight on the mechanisms of neurostimulation, by demonstrating that tACS increases both power and coherence at a neural network's resonant frequency, in a phase-dependent manner.

I. INTRODUCTION

The human brain coordinates firing of neural networks to perform basic cognitive functions. As a result of this neuronal firing, oscillatory electrical activity can be observed on the surface of the scalp. However, it is unknown whether these neural oscillations are functionally significant or an epiphenomenon of cognitive tasks. One way to address this uncertainty is via neuromodulatory techniques, which can test whether neural oscillations causally impact cognitive tasks. Transcranial alternating current stimulation (tACS) is a non-invasive neuromodulation technique that aims to replicate the effects of endogenous oscillations by applying electrical current through the scalp [1]. Past studies found that tACS can modulate attention [2], [3], working memory [4], and speech perception [5]. In auditory spatial attention tasks, 10-Hz alpha waves appear in the parietal cortex ipsilateral to the side of attention. Applying alpha oscillations to the contralateral side has been shown to disrupt attention [2], [3]. However, these studies ignored the inter-subject variability of peak oscillatory alpha power, potentially rendering the neuromodulatory effects of a fixed-frequency tACS less effective due to frequency mismatch between

endogenous oscillations and the externally applied current [6]. Indeed, tACS studies investigating alpha oscillations have demonstrated the importance of stimulating subjects at their individual peak alpha power in order to elicit the strongest stimulation effects [7]. Other mechanisms of tACS have been observed other than matching the frequency of a cognitively relevant brain oscillation. Changing the phase of stimulation relative to syllable onset has also been shown to produce behavioral differences in the perception of the presented syllable, potentially through phasic interactions of the external current and endogenous oscillations [5]. tACS also alters long-range neural connectivity in alpha that arises between multiple brain regions during spatial attention [8]. Despite the many experiments demonstrating behavioral differences after applying tACS, the exact mechanisms by which tACS operates is not well understood [1].

To replicate and expand on these experimental findings, we implemented a biologically plausible Jansen and Rit neural mass model (JRNMM) to simulate neural network dynamics [9]–[11]. The JRNMM treats a cortical column as a dampened oscillator composed of subpopulations of neurons (excitatory interneurons, inhibitory interneurons, and PCs). We instantiated two cortical columns with long-range connections, which allowed us to answer questions about how stimulation between regions impacted long-range connectivity, a question unanswered by the previous modeling studies [12], [13]. Using this double column neural mass model, we replicated the experimental finding that stimulation at the resonant frequencies boosted stimulation effects. We also investigated if the phase of stimulation relative to endogenous oscillations, as well as the phase of stimulation between cortical columns, impacted the neuronal dynamics of the model. Finally, we investigated the impact of tACS on connectivity between interacting brain regions, an effect previous work has not addressed.

II. METHODS

A. Jansen and Ritt neural mass model

A single-column JRNMM treats a cortical source as a combination of excitatory interneurons, PCs, and inhibitory interneurons. These subpopulations are connected to mimic biological observations:

- Extrinsic inputs drive the excitatory interneurons.
- Excitatory interneurons depolarize the PCs.
- Inhibitory interneurons hyperpolarize the PCs.
- PCs depolarize the excitatory and inhibitory interneurons.

*This work was supported by grant from the N00014-18-1-2069 Office of Naval Research.

¹Alexander Pei (email: apei2@andrew.cmu.edu) and Barbara G. Shinn-Cunningham (email: bgsc@andrew.cmu.edu) are with the Department of Electrical and Computer Engineering, Carnegie Mellon University, Pittsburgh, PA 15213, USA

²Barbara Shinn-Cunningham is also with the Neuroscience Institute, Carnegie Mellon University, Pittsburgh, PA 15213, USA

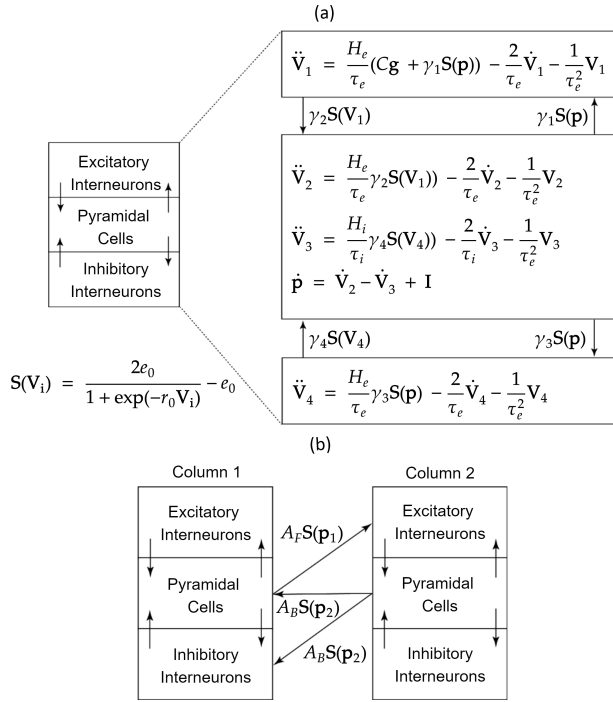


Fig. 1: (a) The state equations for a single column model. V_i denotes the membrane potential of the i^{th} subpopulation ($i = 1$ excitatory interneuron membrane potential, $i = 2$ depolarizing PC membrane potential, $i = 3$ hyperpolarizing PC membrane potential, $i = 4$ inhibitory interneuron membrane potential). p is the net PC membrane depolarization. $S(V_i)$ is the sigmoid function which transforms the membrane potential from one region to a firing rate input to another region. I is the current injected into the model. (b) Dual column model with forward and backward connections between populations. p_1 and p_2 are the PC membrane potentials of column 1 and 2.

TABLE I: Model hyperparameters

Parameter	Description	Value
H_e, H_i	Max amplitude of post-synaptic potential	3.25, 29.3 (mV)
τ_e, τ_i	Lumped time constants of dendritic delays	10, 15 (s^{-1})
e_0	Max firing rate of neural population	2.5 (s^{-1})
r_0	Steepness of the sigmoid function	0.56 (mV^{-1})
$\gamma_1 \dots \gamma_4$	Number of synapses in neural population	50, 40, 12, 12
C	Connectivity scalar for extrinsic inputs	1000

Each subpopulation is modeled by a set of nonlinear second-order differential equations, where the states of the system parameterize a subpopulation's membrane potential. Connected subpopulations are able to influence one another through intrinsic connections. A sigmoid function converts membrane potentials from one subpopulation to an average firing rate input into another subpopulation, and the net depolarization is the sum of all incoming firing rates. The intrinsic parameter γ determines the strength of these connections. The observable output of the JRNMM is the PC depolarization, which dominates EEG signals on the scalp.

The single-column JRNMM can be expanded into a two-column model with the inclusion of extrinsic inputs between columns as seen in Fig. 1. Similar to the intrinsic connections, extrinsic connections input an average firing rate into the target population. In this model, we included forward connections A_F from column 1 to column 2, which target the excitatory interneurons and mimic a bottom-up interaction. Backward connections A_B were placed from column 2 to

column 1, which target both inhibitory interneurons and PCs, and mimic a top-down interaction. The extrinsic connections had a delay of 0.01 ms to simulate conduction delays between regions. Current stimulation was input to only the PC layer due to their net orthogonal orientation to the scalp aligning with the electric field of the applied current, and was summed directly into the first time derivative of the membrane potential, which is proportional to the PC membrane current [12].

The differential equations were integrated and solved using Matlab Simulink with a time-step of 0.001 s. Power and coherence spectra were calculated using the Matlab toolbox Fieldtrip [14].

III. RESULTS

A. Model with AC stimulation

Two cortical columns were instantiated using the model parameters described in Table 1. The forward and backward connections were set to $A_F = 5$ and $A_B = 20$. With these connections, one region exerts a bottom-up effect on the region, which itself provides top-down feedback to the other column. The extrinsic input g was set to be Gaussian random noise with $\sigma = 0.05$ as in [11], to stochastically drive both columns. Each simulation was run for 10 seconds; simulations were repeated for 100 trials with different random noise seeds for each trial. Fig. 2 shows a single trial of the PC output from both columns, as well as the power spectral density (PSD) with a peak power around 4 Hz. The model was then stimulated with AC from 0 to 20 Hz with steps of 0.5 Hz and an amplitude of 2 mA.

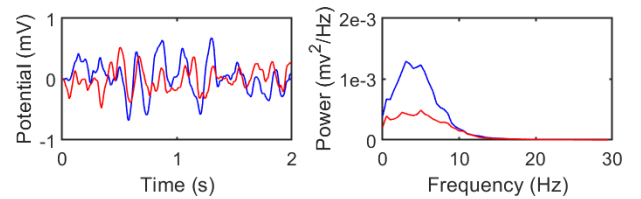


Fig. 2: An example single trial of the simulation. (Left) Time course of the PC membrane depolarization of column 1 (blue) and column 2 (red). (Right) Power spectral density of both PC columns.

Fig. 3 shows the power and coherence spectra at all of the stimulation frequencies. A cluster-based permutation test to determine the significant effects of stimulation on power and coherence was performed on all of the stimulation frequencies [15], [16]. Significant differences were found at all stimulation frequencies for the PSD, but only near the model resonant frequencies for coherence spectra. This was assessed by finding that the observed test statistic was greater than the test statistics of 100 permutations of the simulation labels, ensuring that $p < 0.01$. Upon inspection, it appears that tACS at a frequency near the resonant frequency has the largest effects on power and coherence changes. This is supported by Fig. 4, which shows the difference in power and coherence in the network at the stimulation frequency with and without stimulation, plotted as a function of the stimulation frequency; peaks occur near the network resonant frequencies, highlighted in aqua.

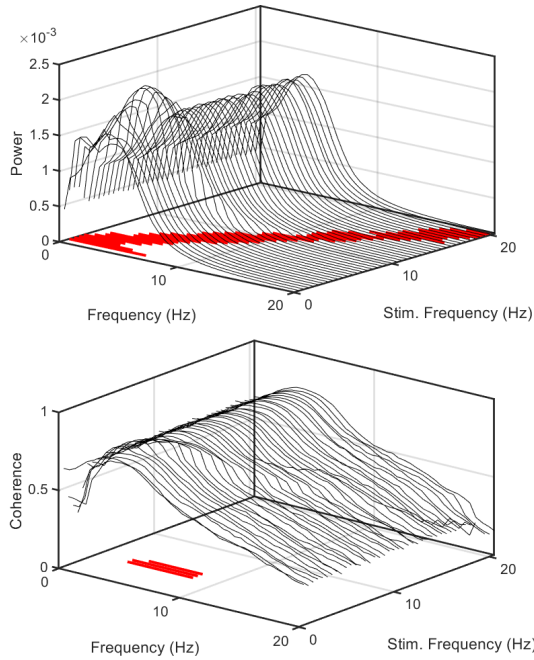


Fig. 3: Power (top) and coherence (bottom) spectra with all stimulation frequencies. The red bar is the largest cluster of p-values, based on adjacent frequency values, for the test statistic (t-test for power, Z-test for coherence), for each of the stimulation frequencies.

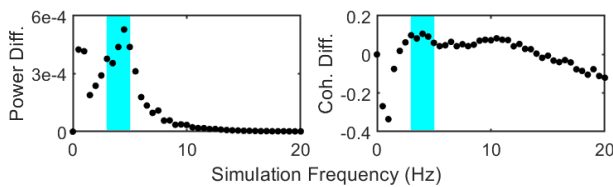


Fig. 4: Difference in power (left) and coherence (right) between no stimulation and with stimulation, at the stimulation frequency, as a function of stimulation frequency. The highlighted region indicates ± 0.5 Hz around the resonant frequency. Coherence was Fisher Z-transformed prior to calculating the difference.

B. Varying onset of stimulation

In the second experiment, the same model in Result A was used, except the current stimulation amplitude was set to 10 mA at 4 Hz to strongly drive the dynamics of both the PC layers, and $A_F = A_B = 50$ to create strong oscillations between the columns. In this experiment, the phase onset of the stimulation relative to the start of the trial was varied. For each simulation, the AC started at 1.5 seconds, plus some delay. The delay ranged from 0 to 1 second, with time steps of 0.01 seconds. The same random noise seed was maintained across trials in order to keep the endogenous oscillations the same. Fig. 5 shows a diagram of the experiment setup. Instantaneous 4 Hz power plots of PC 1 for varying onset phases can be seen in Fig. 6. The entrainment time, defined as how long the oscillatory power took to reach the average power at the last time step, was calculated for each of the phase delays. To determine if constructive or destructive interference was occurring between the membrane current of the PC layer and the AC stimulation, we plotted the average energy of the PC 1 membrane current (\hat{p}) against the entrainment time in

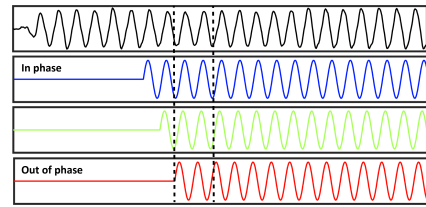


Fig. 5: Diagram of experiment 2. The top most plot shows the endogenous membrane currents of the PC layer \hat{p} over time. The three subsequent plots show varying delays for the onset of the AC stimulation, which are summed together with the PC membrane currents. 50 ms after the current stimulation starts, the average energy is calculated to determine the amount and type of interference between exogenous and endogenous oscillations. The color of the stimulation plots correspond to the color bar in Fig. 6

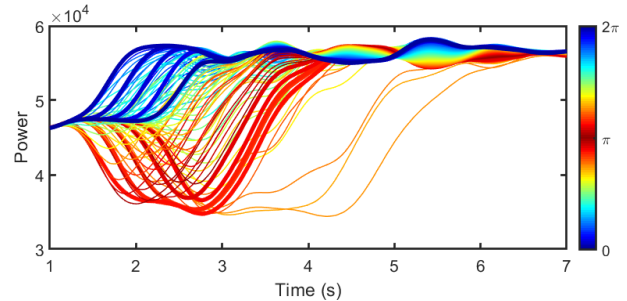


Fig. 6: Instantaneous power calculated at 4 Hz of the PC layer 1 at varying phase shifts. The onset of stimulation occurred at 1.5 seconds, plus some delay. The phase shift above was calculated as $2\pi f dt$, where $f = 4$ and dt is a multiple of 0.01 seconds. The phases were wrapped between zero and 2π . Five of the traces near 2π phase shifts and five traces near π phase shifts are bolded, and all correspond to integer multiples of 2π and π respectively. It is important to note that the longer entrainment observed times at π phase shifts is coincidental; this observation could have been seen at 2π phase shifts if the stimulation began at $1.5 + \pi$. What is important here is the dependency of AC phase shifts and entrainment times as a whole, and not the particular values on the color bar axis.

Fig. 7.

C. Stimulating two columns at different phases

In the final experiment, the two cortical columns were stimulated with different phases with respect to each other. The AC stimulation injected to both PC columns was 4 Hz (at the intrinsic resonant frequency) with an amplitude of 2 mA. The onset of the AC for PC 1 was fixed to start at 1 second, while the onset of the AC for PC 2 was 1 second plus multiples of 0.01 seconds, up to a maximum delay of 1 second. The peak power and coherence at 4 Hz was plotted against the different phase shifts in Fig. 8.

IV. DISCUSSION & CONCLUSIONS

To investigate the mechanisms of alternating current stimulation, we simulated neuronal dynamics in a Jansen and Rit neural mass model injected with alternating current. Two cortical columns were instantiated and connected with forward and backward connections to simulate long-range cortical connections. Without alternating current injected, the model had a unimodal peak frequency at 4 Hz that spanned 0.5 to 20 Hz frequency power. Coherence followed a similar pattern with a peak coherence at 4 Hz. Alternating current injected to the membrane currents of the neuronal subpopulations increased PC depolarization oscillatory power and coherence at the stimulation frequency. The change in power was

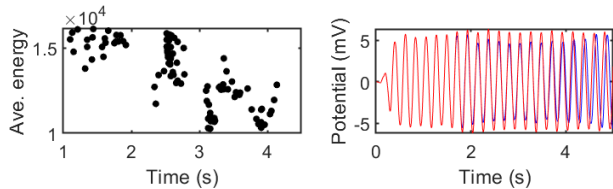


Fig. 7: (Left) Average energy, from the start of stimulation and 50 ms after, of the membrane current \hat{p}_1 plotted against the entrainment time. The energy of the PC membrane current shortly after the onset of stimulation encapsulates the amount of destructive inference between the endogenous current and injected current. (Right) Time series plot of PC layer 1 membrane potential for the trials with the fastest (red) and slowest (blue) entrainment time.

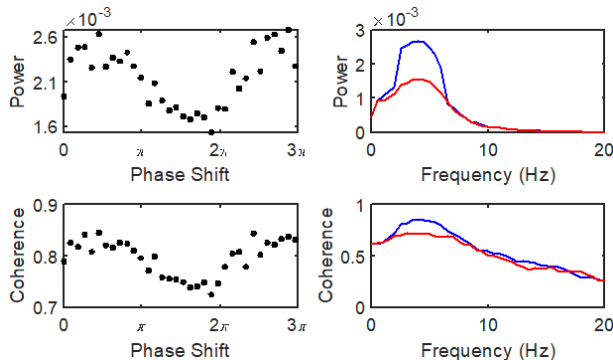


Fig. 8: Peak 4 Hz power (top left) and coherence (bottom left) of PC column 1 for varying phase shifts of the AC stimulation to PC column 2. The PSD (top right) and coherence spectra (bottom right) of the highest (blue) peak 4 Hz power and lowest (red) peak 4 Hz power over all the phase shifts.

greatest near the resonant frequency of the model, consistent with Arnold tongue theories of neurostimulation [12]. The changes in coherence showed a similar trend.

The onset delay of stimulation relative to the start of the model dynamics was varied to assess whether constructive or destructive inference occurred with ongoing oscillations of the model. Varying the onset of stimulation did not impact the steady-state response of the model, but resulted in longer entrainment times for certain phase delays. The longer entrainment times could be explained by the destructive interference occurring between the injected current and the endogenous membrane currents for those stimulation phases.

A few studies have investigated stimulation of multiple brain regions to increase functional connectivity [4]. We demonstrated that varying the phase delay between cortical columns impacted the peak resonant power of the model. This also affected coherence between the two columns, which suggests that increased functional connectivity between regions depends on the phase of stimulation, which in turn leads to increased or decreased peak oscillatory power.

Depending on the validity of the Jansen and Rit neural mass model, these results will require extra consideration from experimenters when designing stimulation paradigms in human subjects. For instance, stimulation effects will be greater if subjects are stimulated at their own individual resonant frequency, which varies between individuals [7]. Additionally, experimenters may need to consider the phase of stimulation, especially in tasks with transient bursts of event-related tACS that do not necessarily reach steady-state dynamics in a brief period of time. One last consideration

is for multi-region stimulation protocols. As shown in our results, large differences of up to 20% in peak power are seen between the worst and best phase offsets. This could vary as a function of distance between electrode sites, and requires additional investigation in human and animal studies.

REFERENCES

- [1] A. J. Woods, A. Antal, M. Bikson, P. S. Boggio, A. R. Brunoni, P. Celnik, L. G. Cohen, F. Fregni, C. S. Herrmann, E. S. Kappenman, H. Knotkova, D. Liebetanz, C. Miniussi, P. C. Miranda, W. Paulus, A. Priori, D. Reato, C. Stagg, N. Wenderoth, and M. A. Nitsche, "A technical guide to tDCS, and related non-invasive brain stimulation tools," pp. 1031–1048, feb 2016.
- [2] Y. Deng, R. M. Reinhart, I. Choi, and B. Shinn-Cunningham, "Causal links between parietal alpha activity and spatial auditory attention," *eLife*, vol. 8, nov 2019.
- [3] M. Wöstmann, J. Vosskuhl, J. Obleser, and C. S. Herrmann, "Opposite effects of lateralised transcranial alpha versus gamma stimulation on auditory spatial attention," *Brain Stimulation*, vol. 11, no. 4, pp. 752–758, jul 2018.
- [4] R. M. Reinhart and J. A. Nguyen, "Working memory revived in older adults by synchronizing rhythmic brain circuits," *Nature Neuroscience*, vol. 22, no. 5, pp. 820–827, may 2019. [Online]. Available: <https://doi.org/10.1038/s41593-019-0371-x>
- [5] T. Neuling, S. Rach, S. Wagner, C. H. Wolters, and C. S. Herrmann, "Good vibrations: Oscillatory phase shapes perception," *NeuroImage*, vol. 63, no. 2, pp. 771–778, nov 2012.
- [6] R. Gulbinaite, T. Van Viegen, M. Wieling, M. X. Cohen, and R. Vanrullen, "Individual Alpha Peak Frequency Predicts 10 Hz Flicker Effects on Selective Attention," *The Journal of Neuroscience*, vol. 37, no. 42, p. 10173, oct 2017. [Online]. Available: <https://www.ncbi.nlm.nih.gov/pmc/articles/PMC6596538/>
- [7] F. H. Kasten, K. Duecker, M. C. Maack, A. Meiser, and C. S. Herrmann, "Integrating electric field modeling and neuroimaging to explain inter-individual variability of tACS effects," *Nature Communications*, vol. 10, no. 1, pp. 1–11, dec 2019. [Online]. Available: <https://doi.org/10.1038/s41467-019-13417-6>
- [8] M. R. van Schouwenburg, T. P. Zanto, and A. Gazzaley, "Spatial attention and the effects of frontoparietal alpha band stimulation," *Frontiers in Human Neuroscience*, vol. 10, p. 658, jan 2017. [Online]. Available: www.frontiersin.org
- [9] B. H. Jansen and V. G. Rit, "Electroencephalogram and visual evoked potential generation in a mathematical model of coupled cortical columns," *Biological Cybernetics*, vol. 73, no. 4, pp. 357–366, sep 1995. [Online]. Available: <https://link.springer.com/article/10.1007/BF00199471>
- [10] O. David and K. J. Friston, "A neural mass model for MEG/EEG: Coupling and neuronal dynamics," *NeuroImage*, vol. 20, no. 3, pp. 1743–1755, nov 2003.
- [11] O. David, L. Harrison, and K. J. Friston, "Modelling event-related responses in the brain," *NeuroImage*, vol. 25, no. 3, pp. 756–770, apr 2005.
- [12] M. M. Ali, K. K. Sellers, and F. Fröhlich, "Transcranial alternating current stimulation modulates large-scale cortical network activity by network resonance," *Journal of Neuroscience*, vol. 33, no. 27, pp. 11262–11275, jul 2013. [Online]. Available: <https://www.jneurosci.org/content/33/27/11262>
- [13] C. Cakan and K. Obermayer, "Biophysically grounded mean-field models of neural populations under electrical stimulation," *PLoS Computational Biology*, vol. 16, no. 4, p. e1007822, apr 2020. [Online]. Available: <https://doi.org/10.1371/journal.pcbi.1007822.g001>
- [14] R. Oostenveld, P. Fries, E. Maris, and J. M. Schoffelen, "FieldTrip: Open source software for advanced analysis of MEG, EEG, and invasive electrophysiological data," *Computational Intelligence and Neuroscience*, vol. 2011, 2011.
- [15] E. Maris, J. M. Schoffelen, and P. Fries, "Nonparametric statistical testing of coherence differences," *Journal of Neuroscience Methods*, vol. 163, no. 1, pp. 161–175, jun 2007.
- [16] E. Maris and R. Oostenveld, "Nonparametric statistical testing of EEG- and MEG-data," *Journal of Neuroscience Methods*, vol. 164, no. 1, pp. 177–190, aug 2007.